nature chemical biology

ARTICLE

PUBLISHED ONLINE: 17 JUNE 2012 | DOI: 10.1038/NCHEMBIO.1002

Phenylalanine assembly into toxic fibrils suggests amyloid etiology in phenylketonuria

Lihi Adler-Abramovich[1], Lilach Vaks[1], Ohad Carny[1], Dorit Trudler[2,3], Andrea Magno[4], Amedeo Caflisch[4], Dan Frenkel[2,3] & Ehud Gazit[1]*

Phenylketonuria (PKU) is characterized by phenylalanine accumulation and progressive mental retardation caused by an unknown mechanism. We demonstrate that at pathological concentrations, phenylalanine self-assembles into fibrils with amyloid-like morphology and well-ordered electron diffraction. These assemblies are specifically recognized by antibodies, show cytotoxicity that can be neutralized by the antibodies and are present in the hippocampus of model mice and in parietal cortex brain tissue from individuals with PKU. This is, to our knowledge, the first demonstration that a single amino acid can form amyloid-like deposits, suggesting a new amyloidosis-like etiology for PKU.

Individuals with PKU can have mental retardation, epilepsy, organ damage and unusual posture, and the molecular mechanisms causing these are largely obscure. PKU is an autosomal recessive disorder, caused by mutations in the gene encoding phenylalanine hydroxylase (PAH) located on chromosome 12. Mutations in both alleles of the gene result in remarkably high concentrations of phenylalanine[1,2]. In untreated patients, millimolar concentrations of phenylalanine accumulate in the plasma, cerebrospinal fluid and brain tissue[3,4]. The inclusion of PKU diagnosis in newborn screening programs, by semiquantitative methods such as the Guthrie test or modern analytical tools that measure the blood concentrations of phenylalanine, allows early diagnosis of affected individuals. This permits treatment with a phenylalanine-restricted diet before the onset of clinical symptoms. A high percentage of individuals with PKU have blood phenylalanine concentrations that are above target ranges, particularly in teenagers and adults, indicating inadequate compliance to the strict diet[5]. In most of the previous studies, phenylalanine was considered to act as a neurotoxin, although the precise mechanism underlying its neurological effects still needed to be deciphered[2].

In the past decade, the role of peptide and protein aggregation in many pathological disorders was revealed. Specific attention was drawn to the formation of ordered amyloid fibrils. It was clearly demonstrated that amyloid fibrils or their early intermediates are associated with a diverse group of diseases of unrelated etiology, including Alzheimer's disease, type II diabetes and prion disorders. Despite their formation by a diverse and structurally unrelated group of proteins, all amyloid fibrils share similar biophysical and structural properties[6,7]. A variety of structural and biophysical studies indicate that aromatic residues are important in the acceleration of the amyloidogenic process and the stabilization of amyloidal structure. Although aromatic interactions are not crucial for the process of amyloid formation, they can substantially accelerate it, affect the morphology of the assemblies and reduce the minimal association concentrations[8–11]. It was previously shown that very short aromatic peptide fragments, as short as penta- and tetrapeptides, can form typical amyloid fibrils that share the same biophysical and structural properties of the assemblies formed by much larger polypeptides[9,12]. Furthermore, diphenylalanine peptide was shown to form well-ordered nanotubular assemblies by itself, with some amyloid-like structural signatures[13]. This short peptide represents the core recognition motif within the β-amyloid polypeptide, which forms amyloid plaques in Alzheimer's disease. The two phenylalanine residues (Phe19 and Phe20) in the β-amyloid peptide were suggested to mediate the intermolecular interaction between polypeptide chains. This suggestion was further substantiated by the use of phenylalanine residues as a key component of peptide-based inhibitors of β-amyloid fibril formation[14,15].

In spite of the extensive work that is performed on short peptide fragments, no study has yet examined the association between single amino acids. Inspired by the frequent occurrence of phenylalanine residues in short amyloid-forming peptides[9] and by the efficient formation of nanotubes by the self-assembly of the diphenylalanine peptide[13], we explored the ability of phenylalanine to form amyloid-like nanofibrillar structures under millimolar concentrations. As discussed below, our finding may lead to a better understanding of the pathology caused by the accumulation of phenylalanine, which can reach millimolar concentrations in individuals with PKU[1,16] and lead to new approaches of treatment for this disease.

RESULTS

Biophysical characterization of phenylalanine assemblies

We examined the ability of the aromatic amino acid phenylalanine to form ordered assemblies under pathologically relevant concentrations. We observed that phenylalanine by itself, at millimolar concentrations, self-assembles to form amyloid-like nanofibrillar structures. To study the process and outcome of phenylalanine fibril formation, we applied a series of biophysical and biological assays. Transmission electron microscopy (TEM) analysis of phenylalanine at the millimolar-concentration range indicated the occurrence of well-ordered and elongated assemblies (**Fig. 1a**). Scanning electron microscopy (SEM) was also used to study the three-dimensional structures of the fibrils (**Supplementary Results**, **Supplementary Fig. 1a**), and environmental SEM (ESEM) was used to study fibrillar structures in a humid environment (**Supplementary Fig. 1b**). Both SEM and ESEM micrographs

[1]Department of Molecular Microbiology and Biotechnology, George S. Wise Faculty of Life Sciences, Tel Aviv University, Tel Aviv, Israel. [2]Department of Neurobiology, George S. Wise Faculty of Life Sciences, Tel Aviv University, Tel Aviv, Israel. [3]Sagol School of Neuroscience, Tel Aviv University, Tel Aviv, Israel. [4]Department of Biochemistry, University of Zurich, Zurich, Switzerland. *e-mail: ehudg@post.tau.ac.il

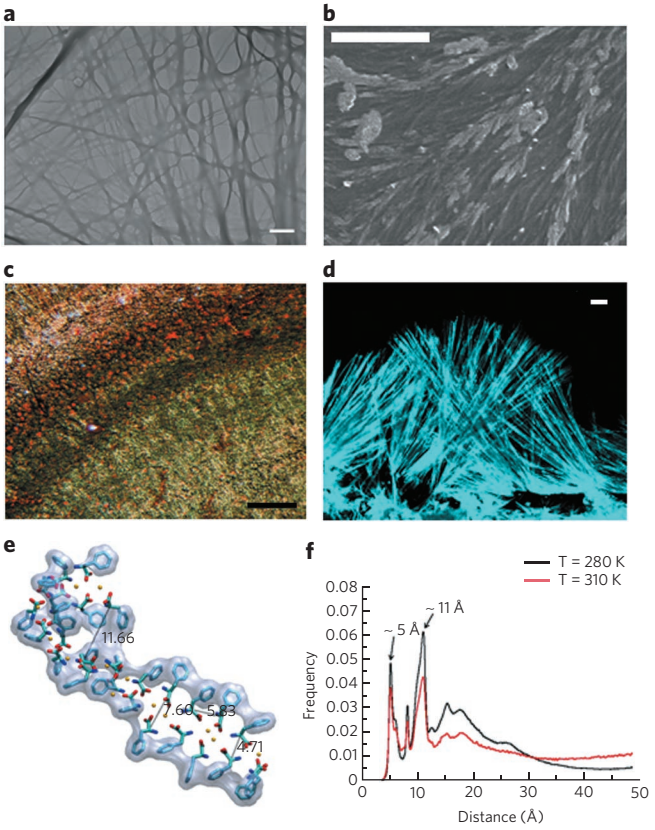

Figure 1 | The single aromatic amino acid, phenylalanine, self-assembles into supramolecular fibrillar structures. (**a**) TEM images of elongated phenylalanine fibrils. Scale bar is 1 µm. (**b**) SEM images of phenylalanine fibrils in human serum. Scale bar is 20 µm. (**c**) Microscopic examination under polarized light following Congo red staining of phenylalanine fibrils. Scale bar is 500 µm. (**d**) Confocal microscopy image of fibrils dyed with ThT. Scale bar is 10 µm. (**e**) Representative snapshot of the filamentous structure obtained by molecular dynamics simulations started with 27 monodisperse phenylalanine molecules (cyan) at high pH in the presence of counterions (yellow spheres). The tight packing of the aromatic rings is emphasized by their van der Waals envelope (gray surface). (**f**) Distribution of distances between pairs of atoms in different phenylalanine molecules in the aggregates obtained by molecular dynamics simulations. The distances between the center of mass of all pairs of the 27 phenylalanines were used for these histograms, and quantitatively similar histograms were obtained using distances between atoms instead of those between center of masses. The very similar distributions at 280 K (black) and 310 K (red) show that the ordered aggregates of phenylalanine are essentially the same in this temperature range and that the simulations have reached convergence.

showed areas covered with discrete assemblies, demonstrating that the assemblies are relatively homogeneous and are evidently discrete entities with a persistence length on the order of a few micrometers. We have also demonstrated by SEM analysis that phenylalanine fibrillar structures are formed in human serum, a more physiologically relevant environment (**Fig. 1b**). Both HPLC and NMR analysis clearly indicated that no covalent bonds were formed between the phenylalanine monomers and that the highly ordered fibrils are supramolecular assemblies (**Supplementary Fig. 1c**). All of these data imply that phenylalanine assembles into amyloid-like structures and that this assembly can take place under pathologically relevant conditions.

Another characteristic of amyloid fibrils is the presence of typical yellow-green birefringence upon staining with Congo red, visualized by microscopic examination under cross-polarized light. The birefringence results from the high order of the assemblies at the molecular level. Thus, we examined the phenylalanine assemblies using Congo red staining to gain further information on their internal order. Upon microscopic exanimation, we observed a characteristic birefringence similar to that of amyloid fibrils (**Fig. 1c**). An additional common method for quantitative assessment of amyloid fibrils is the thioflavin T (ThT) fluorescence assay, which reflects the change in the dye's fluorescence upon interaction with ordered assemblies. We used the ThT fluorescence assay to visualize the phenylalanine fibrils and observed an excitation shift typical of amyloid fibril binding of ThT. Fluorescence confocal microscopy analysis of the ThT-stained fibrils showed the presence of elongated ordered structures (**Fig. 1d**).

Another method of confirming the degree of order of fibrillar structures is the use of electron diffraction. This was previously used to probe the ultrastructure of amyloid fibrils[10,17]. Indeed, in the case of the phenylalanine fibril, electron diffraction studies also gave a strong indication to the high organization of the assemblies. An electron diffraction pattern of a single fibril was consistent with a unit cell of $a = 11.63 \pm 0.27$ Å, $c = 4.6 \pm 0.06$ Å (for $n = 5$ measurements), where a is oriented normal to the long axis of the crystal, and c is along the fiber axis (**Supplementary Fig. 1d**).

Molecular dynamics simulations[18] with a generalized Born implicit solvent model[19] were carried out to shed light on the structures of the early aggregates of phenylalanine. Multiple microsecond-long simulations were started with 27 monodispersed phenylalanine molecules at different pH values and in the presence or absence of counterions. Ordered aggregation was observed at some but not all conditions. At high pH (that is, neutral amino group and negatively charged carboxy group) in the presence of counterions, filamentous aggregates were observed in high concentrations and at all temperature values (**Fig. 1e**). Analysis of the ensemble of self-assembled structures yielded a distribution of interatomic distances with two peaks at about 5 Å and 11 Å (**Fig. 1f**), which correspond to the distance between neighboring phenylalanines and the laminal spacing, respectively (**Fig. 1e**). Pairs of neighboring phenylalanines are involved in direct hydrogen bonds or salt-bridged polar interactions. Notably, the distribution of distances is in agreement with the aforementioned electron diffraction pattern.

Taken together, the results of the set of experimental techniques and atomistic simulations further confirm that the high degree of structural order of the phenylalanine fibrillar assemblies is not the product of irregular aggregation. In this sense, they have characteristics similar to those of amyloid fibrillar deposits. We conclude that the fibrils formed by phenylalanine closely resemble amyloid structures, as confirmed by all of the physical assays used.

Cytotoxicity of phenylalanine assemblies

We examined whether, like many amyloid structures, phenylalanine assemblies have a cytotoxic effect. This was examined at a physiological range of concentrations, similar to those detected in untreated PKU individuals, by *in vitro* cellular viability experiments. To this end, elevated concentrations of phenylalanine ranging from 0.1 µM to 15 mM were added to cultured PC12 cell line (**Fig. 2a**) and to cultured Chinese hamster ovary (CHO) cells (**Supplementary Fig. 2a**). The phenylalanine fibrils, at millimolar concentrations, had a toxic effect on the cells as measured by the 3-(4,5-dimethylthiazolyl-2)-2,5-diphenyltetrazolium bromide (MTT) assay (**Fig. 2a**). In the presence of 1.8 mM phenylalanine, cell viability decreased to approximately 80%. Moreover, in the presence of 7.5 mM phenylalanine, the cells' viability was approximately 65% (**Fig. 2a**), suggesting a dose-dependent response. Our assay was performed at much shorter time scales than those for disease progression, which may account for our use of slightly elevated concentrations compared to those typically found in individuals with PKU. It is also possible

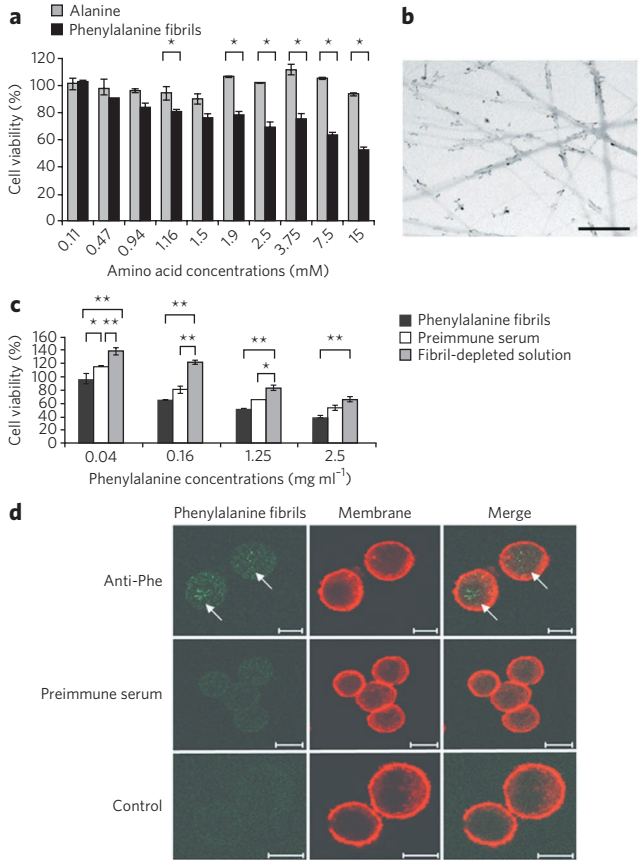

Figure 2 | Specific antibodies against phenylalanine fibrils and the toxic effect and interaction of phenylalanine fibrillar structures with cell cultures. (**a**) Cell viability was determined using the MTT assay. The PC12 cell line was maintained in the presence of phenylalanine fibrils (black bars) or the control amino acid, alanine (gray bars). $^{*}P < 0.05$. (**b**) TEM micrographs of phenylalanine fibrils, visualized using antibodies that were specifically bound to phenylalanine fibrils and then were marked with a secondary antibody conjugated to 18-nm gold particles. Scale bar is 2 μm. (**c**) Cell viability was determined using the MTT assay, CHO cell cultures were maintained in the presence of an increasing amount of phenylalanine fibrils (black bars) or immunoprecipitated (IP) solutions of phenylalanine depleted of fibrils (gray bars). As control, phenylalanine fibrils were also incubated with preimmune serum (white bars). $^{*}P < 0.05$; $^{**}P < 0.001$. Results for **a** and **c** are presented as mean ± s.e.m. (**d**) CHO cell cultures were incubated with phenylalanine fibrils, fixed, and then incubated with anti-Phe and stained using Alexa 488–conjugated antibody (green, marked with arrows). The cell membrane was marked with phalloidin (red). As controls, CHO cell cultures were incubated with phenylalanine fibrils then fixed and incubated with preimmune serum or without primary antibodies. Scale bars are 10 μm.

that such high concentrations of phenylalanine occur pathologically in individuals with PKU, owing to transient local high concentrations of phenylalanine in the brain. Slightly elevated phenylalanine concentrations were used, similarly to the experimental studies of β-amyloid polypeptide, which in Alzheimer's disease occurs at overall cerebral concentrations lower than 10 nM, whereas toxicity studies are performed at the micromolar range[20,21]. Furthermore, alanine, an average-sized amino acid that does not form fibrillar structures at similar concentrations, was used as a negative control in the cytotoxicity assay and, as expected, did not demonstrate a toxic effect (**Fig. 2a**). Thus, it is quite clear that it is not merely the concentration of amino acid monomers but rather the mulitimolecular entity that is the cause of toxicity.

We further assessed the influence of the phenylalanine fibrils on the morphology of CHO cells using SEM. We observed changes in CHO cell morphology following incubation with phenylalanine fibrils. In the absence of phenylalanine fibrils, the cells had an elongated shape (**Supplementary Fig. 2b**,**c**), whereas the phenylalanine-treated cells seemed smaller and rounder (**Supplementary Fig. 2d**,**e**). We observed a very low density of the phenylalanine-treated cells compared to that of the untreated cells. On the basis of these results, we suggest that phenylalanine pathology in individuals with PKU may be due to the cytotoxic effects of fibril formation at millimolar concentrations.

Formation of antibodies against phenylalanine fibrils

One of the key prospects for amyloid disease treatment is the use of antibodies that specifically recognize and clear fibrillar assemblies and not the corresponding monomeric species. To examine whether the phenylalanine fibrils represent a unique immunological entity, we tried to produce specific antibodies against the phenylalanine fibrils. Rabbits were immunized with the fibrils, and their serum was tested for specificity to the assemblies. We employed an immunogold assay to show the antibodies' affinity to the fibrils. As can be observed in the TEM images, the fibrils were specifically marked with gold-labeled secondary antibodies bound to the serum antibodies (**Fig. 2b**). Control analysis of phenylalanine fibrils, marked with preimmune serum or only with gold-labeled secondary antibodies, did not show any specificity to the fibrils (**Supplementary Fig. 3**). Moreover, the specificity of the antibodies was demonstrated, as no cross-reactivity was found when the antibodies were incubated with the Parkinson's α-synuclein amyloid deposits or with diphenylalanine peptide nanotubes[13], and only low binding was observed when the antibodies were added to phenylalanine monomers dissolved in guanidine hydrochloride solution, reflecting their much lower ability to self-assemble. In addition, no binding was observed when preimmune serum was used as a control (**Supplementary Fig. 4**). This observation provides a clear indication for the formation of distinctive and specific immunological epitopes by the self-assembly of phenylalanine, as observed in amyloid disorders.

Immunoprecipitation depleted phenylalanine fibril toxicity

Antibodies against phenylalanine fibrils (anti-Phe fibril) were furthermore used to immunoprecipitate the phenylalanine assemblies from the solution and to assess the contribution of the assemblies to the toxic effect on the cell culture. **Figure 2c** compares the cytotoxic effect of phenylalanine assemblies prior to and following immunoprecipitation. Cells treated with solutions containing phenylalanine assemblies at concentrations of 2.5 mg ml^{-1} and 0.16 mg ml^{-1} showed only 40% and 68% cell viability, respectively; however, after immunoprecipitation, the viability of cells incubated with the solutions was elevated to 66% and 122%, respectively, as measured by the MTT assay (**Fig. 2c**). In addition, the solutions that were incubated with the cells were analyzed using electron microscopy; phenylalanine fibrils were observed in the solution before the immunoprecipitation and were not detected after immunoprecipitation with anti-Phe fibril (**Supplementary Fig. 5**). As a control, cell viability after immunoprecipitation of the phenylalanine fibrils with preimmune serum was analyzed. The viability of the cells incubated with the 2.5 mg ml^{-1} and 0.16 mg ml^{-1} solutions was moderately elevated to 59% and 80%, respectively. The nonspecific preimmune serum showed a notably lower depletion effect in comparison to the specific anti-Phe fibril depletion. The moderate elevation in viability may possibly be due to some sedimentation of the phenylalanine fibrils during the immunoprecipitation procedure. In addition, electron microscopy analysis showed phenylalanine fibrils in the preimmune immunoprecipitated solution, correlating with the results showing low viability (**Supplementary Fig. 5**).

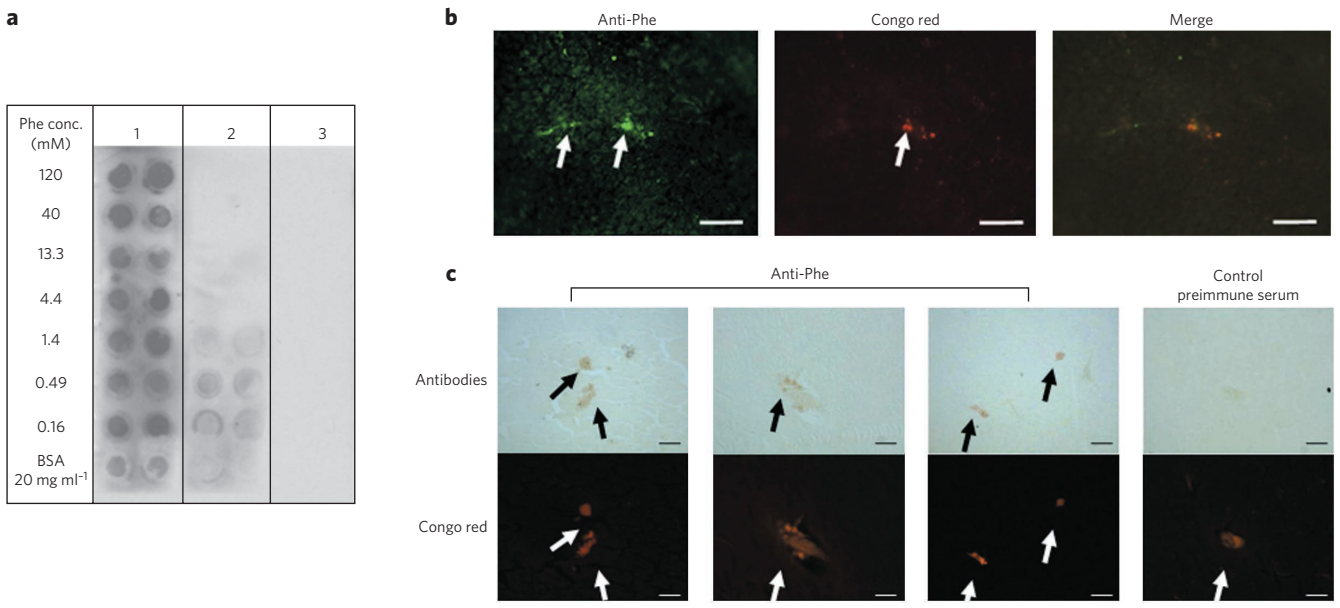

Figure 3 | Dot-blot analysis and histological staining indicates the presence of phenylalanine fibrils in model mice and PKU patient brain tissues. (**a**) Dot-blot analysis of phenylalanine fibrils. Column 1, serum of homozygous mouse (*Pah*^{enu2}) strongly bound the phenylalanine fibrils. Column 2, serum of heterozygous mouse (*Pah*^{enu2}) did not bind the phenylalanine fibrils. Column 3, serum of wild-type mouse did not bind phenylalanine fibrils. (**b**) Histological staining of homozygous *Pah*^{enu2} mouse brain. The 20-μm-thick brain slices were stained with rabbit anti–Phe fibril antibodies and Congo red and then were examined using fluorescent microscopy. The detected amyloid-like plaques showed colocalization of the fluorescent signal obtained from Congo red and antibody staining. (**c**) The brain of an individual with PKU was stained with anti–Phe fibril serum or with preimmune serum, examined using light microscopy and co-stained with Congo red. Phenylalanine-positive depositions were found in the parietal cortex. Scale bars are 100 μm.

Phenylalanine fibrils interact with cells

Moreover, confocal microscopy was used to study the interaction of the fibrils with CHO cells in culture (**Fig. 2d**). Cells were incubated with phenylalanine fibrils following cell fixation and staining with antibody against phenylalanine (anti-Phe) and phalloidin. Analysis of the cells clearly demonstrated that the fibrils could be detected within the cells (**Fig. 2d**) under the conditions in which cytotoxicity is observed (**Fig. 2a**). No such staining could be observed with the preimmune serum (**Fig. 2d**) or without the addition of the primary antibody (**Fig. 2d**).

The presence of phenylalanine fibrils in *Pah*^{enu2} mice

To prove that these assemblies exist *in vivo*, we examined serum samples obtained from a genetic mouse model of PKU (*Pah*^{enu2}), deficient in phenylalanine hydroxylase activity[22]. We were interested in analyzing the presence of anti-Phe fibril, which could indicate the presence of phenylalanine fibril in the PKU mouse model. Using the dot-blot assay, we were able to observe anti-Phe fibril specifically in *Pah*^{enu2} homozygous mouse serum (**Fig. 3a**). Moreover, anti-Phe was not detected in control *Pah*^{enu2} heterozygous mouse serum and in normal mouse serum (**Fig. 3a**). We further examined the presence of phenylalanine fibrils in brain tissue of *Pah*^{enu2} mice. We performed histology staining experiments using Congo red and Phe-specific antibody staining. The histology staining results showed evidence for the presence of amyloid-like plaques in *Pah*^{enu2} mice (**Fig. 3b**). A large number of plaques were specifically detected in the hippocampus and dentate gyrus (**Fig. 3b**), and in proximity to blood vessels (**Supplementary Fig. 6a**). Notably, considerable necrosis and edema in the dentate gyrus were described in previous studies on PKU[23]. In addition, the colocalization of Congo red and anti-Phe staining provides evidence that the plaques consist of amyloid-like phenylalanine fibrils. DAPI staining (nonspecific staining of double-stranded DNA) of plaque sections detected glia cell infiltration to the region (data not shown). In addition, the following four histological staining controls showed no evidence of phenylalanine assemblies**:** (i) homozygous *Pah*^{enu2} mouse brain tissue, stained with antibodies extracted from immunized serum depleted of its Phe fibril–specific antibodies by preincubation with phenylalanine fibrils; (ii) homozygous *Pah*^{enu2} mouse brain tissue, stained with antibodies derived from preimmune serum; (iii) heterozygous *Pah*^{enu2} mouse brain tissue stained with anti-Phe; (iv) heterozygous *Pah*^{enu2} mouse brain tissue stained with preimmune serum (**Supplementary Fig. 6b–e**).

Immunohistology of phenylalanine fibrils in PKU patients

We examined the presence of phenylalanine fibrils in the brain tissue of individuals with PKU. We performed histological staining with both anti-Phe fibril and Congo red. As shown in **Figure 3c**, evidence was found for the presence of phenylalanine deposition in the brain tissue using both immunostaining and Congo red staining (**Fig. 3c**). The control sample stained with Congo red showed positive staining; however, the preimmune serum did not recognize this area (**Fig. 3c**, right column). These findings demonstrate the specificity of the anti-Phe fibril. The phenylalanine assemblies' co-staining was mainly detected in the parietal cortex, which was previously suggested to be involved in the pathology of PKU in a rat model, in terms of changes in the structural organization of the cortex and decreased number of dendritic processes[24]. Thus, the phenylalanine assemblies not only are clear supramolecular entities but also are most relevant to the disease, as determined by the mouse model experiments.

DISCUSSION

The current study presents a new paradigm to explain the pathology of PKU and suggest new routes for potential therapy. Our study indicates, for what is to our knowledge the first time, the ability of phenylalanine, a single amino acid, to form well-ordered fibrillar assemblies at the nano scale. These assemblies are not irregular aggregates,

as they have typical fibrillar morphology, characteristic birefringence, ThT fluorescence patterns and, above all, clear electron diffraction patterns. In all of these aspects, the properties of these fibrils highly resemble those of amyloid assemblies, which are related to numerous pathological disorders. The formed structures not only are ordered as amyloid fibrils but also have strong and clear cytotoxic activities, as other amyloid assemblies do[25,26]. Moreover, the formation of phenylalanine aggregates could be detected in the brain of PKU model mice and individuals with PKU using Phe-specific antibodies. These findings suggest that PKU is closely related to the family of amyloid-related diseases and might have similar etiology. Moreover, the phenylalanine fibrils represent a distinct immunological entity, like amyloid assemblies, and many concepts and experimental studies that are used for the development of immunological treatment for amyloid diseases may also be used in this case[27,28].

METHODS

Materials. Amino acids were purchase from Sigma (purity ≥98%). Fresh stock solutions were prepared by dissolving the amino acid in double-distilled H_2O (ddH_2O), PBS or DMEM (Beit Haemek) or human serum at various concentrations ranging from 6 µM to 120 mM.

TEM. Phenylalanine was dissolved in ddH_2O to a concentration of 6 mM and incubated at 25 °C for 2 h. A 10-µl aliquot of this solution was placed on 400-mesh copper grids. After 1 min, excess fluids were removed. For negative staining, the grid was stained with 2% (w/v) uranyl acetate in water, and after 2 min excess fluids were removed from the grid. Samples were viewed using a JEOL 1200EX electron microscope operating at 80 kV.

Molecular dynamics simulations. Molecular dynamics simulations with a generalized Born implicit solvent model[19] were carried out. Multiple microsecond-long simulations were started with 27 monodispersed phenylalanine molecules at different pH values and in the presence or absence of counterions. Four different concentrations of phenylalanine (1 mM, 6 mM, 30 mM and 100 mM) and three temperature values (280 K, 300 K and 310 K) were used.

Antibodies formation. Phenylalanine was dissolved in ddH_2O at a concentration of 120 mM to form fibrils; rabbits were immunized five times subcutaneously at 14-d intervals with the fibrils and Freund's adjuvants. Seven days after each injection, the rabbits were bled, and their serum was tested using dot-blot analysis.

Rabbit antibody immunotesting using TEM analysis. The immunolabeling was visualized using goat anti-rabbit conjugated with 18-nm gold (Jackson ImmunoResearch; catalog no. 111-215-144 1:20). Phenylalanine was adhered to the copper grid as described in the TEM section. Then, the grid was blocked with 1% (w/v) BSA and 3% (w/v) goat serum for 30 min. Samples were incubated with the serum diluted 1:200 in PBS in 1% milk for 30 min, washed five times with 0.1% BSA, then incubated with the secondary antibody for 30 min and similarly washed. Samples were viewed using a JEOL 1200EX electron microscope operating at 80 kV.

Immunoprecipitation and cell cytotoxicity experiments. Phenylalanine solutions at concentrations of 2.5 mg ml^{-1}, 1.25 mg ml^{-1}, 0.16 mg ml^{-1} and 0.04 mg ml^{-1} were either incubated with CHO cells or immunoprecipitate, and then the solutions, with or without the fibrils, were incubated with CHO cells according to the cell cytotoxicity experiments detailed in the **Supplementary Methods**. Samples were immunoprecipitated with either anti-Phe fibril or preimmune serum (1:10) overnight at 4 °C (previously purified on protein A column, in PBS plus 2% (w/v) BSA).

Interaction of phenylalanine fibrils with CHO cells. The interaction of the fibrils with cells in culture was visualized by immunocytochemistry staining. Cells were seeded on a cover slip in a 24-well plate. Cells were washed with PBS and fixed with 4% (v/v) paraformaldehyde (PFA) in PBS for 30 min at 25 °C and then were washed twice with PBS and permeabilized with 0.1% Triton in PBS for 2 min. Following two PBS washes, cells were blocked with 10% (v/v) normal goat serum in 3% **(w/v)** BSA for 30 min and incubated with anti-Phe diluted 1:1,000 and 4 µg ml^{-1} phalloidin (Sigma) for 1 h, followed by an additional hour of incubation with Alexa 488–conjugated goat anti–rabbit IgG (Jackson ImmunoResearch; catalog no: 711-545-152; diluted 1:500). After being thoroughly washed with PBS, cells were mounted using ProLong Antifade (Invitrogen). Images were taken with LSM META confocal microscope (Zeiss).

Congo red staining of brain tissue of *Pah*^{enu2} mice. Fifteen-micrometer coronal brain sections of *Pah*^{enu2} homozygous and heterozygous mice were prepared using cryostat. Brain samples were fixed in 70% (v/v) ethanol for 1 min, washed in ddH_2O for 2 min and stained with previously filtered Congo red solution for 10 min. Following staining, the samples were washed in ddH_2O for 2 min and washed 8–10 times in NaOH-ethanol solution (0.5 ml 1% (w/v) NaOH plus 49.5 ml 50% (v/v) ethanol) until the excess red color disappeared. Finally, the samples were washed in ddH_2O, and the signal was detected using fluorescent microscopy (absorption at 498 nm, emission at 614 nm).

Immunohistological staining of mouse brain tissue. Black and tan, brachyuric (BTBR)-*Pah*^{enu2} brain samples were fixed in 4% PFA (in PBS) for 5 min and washed for 5 min in ddH_2O. The slices were blocked with 2% BSA solution (in PBS) for 20 min, then washed three times in ddH_2O and incubated with rabbit anti-Phe fibril solution, dilution 1:20 (previously purified on a protein A column, in PBS plus 2% (w/v) BSA) for 1 h at 25 °C. Following the incubation, the samples were washed three times in ddH_2O and incubated with goat rabbit-specific secondary antibody conjugated to Alexa F488 (Invitrogen; catalog no. A11008; diluted 1:250). Signal was detected by fluorescent microscope (absorption at 495 nm, emission at 519 nm).

Immunohistological staining of human brain tissue. Brain samples, acquired from the London Neurodegenerative Diseases Brain Bank (part of BrainNet Europe), were fixed in paraffin. Consecutive sections were deparaffinized with xylene, fixed in 4% (v/v) PFA and treated with 0.3% (v/v) H_2O_2 (in PBS). Sections were then heated in citric acid (pH 6) for 5 min and were treated with 0.25% (v/v) Triton X-100 for 3 min. The sections were blocked using 2% (w/v) BSA solution (in PBS) for 20 min, then washed three times in PBS and incubated with rabbit anti-Phe fibril solution, dilution 1:50 (previously purified on protein A column, in PBS plus 2% (w/v) BSA) for 1 h at 25 °C, along with preimmune rabbit serum as control. Following the incubation, the samples were washed 3 times in PBS and incubated with goat rabbit-specific secondary antibody conjugated to biotin (Vector laboratories, BA-1000) diluted 1:250 for 1 h at 25 °C and washed with PBS. Sections were then treated with ABC reagent (Vector Laboratories, Vectastatin ABC kit, PK-6100) and developed with diaminobenzidine and hydrogen peroxide (Vector Laboratories, SK-4100). Signal was detected by light microscope.

Statistical analysis. Two-tailed Student's *t*-test was performed when two groups were compared. The one-way analysis of variance followed by Bonferroni's multiple comparison tests was carried out for multiple samples. Statistical significance was determined at $P < 0.05$.

Received 26 July 2010; accepted 7 May 2012; published online 17 June 2012

References

1. Hanley, W.B. Adult phenylketonuria. *Am. J. Med.* **117**, 590–595 (2004).
2. Surtees, R. & Blau, N. The neurochemistry of phenylketonuria. *Eur. J. Pediatr.* **159** (suppl.), S109–S113 (2000).
3. Choi, T.B. & Pardridge, W.M. Phenylalanine transport at the human blood-brain barrier. Studies with isolated human brain capillaries. *J. Biol. Chem.* **261**, 6536–6541 (1986).
4. Krause, W. *et al.* Biochemical and neuropsychological effects of elevated plasma phenylalanine in patients with treated phenylketonuria. A model for the study of phenylalanine and brain function in man. *J. Clin. Invest.* **75**, 40–48 (1985).
5. MacDonald, A., Gokmen-Ozel, H., van Rijn, M. & Burgard, P. The reality of dietary compliance in the management of phenylketonuria. *J. Inherit. Metab. Dis.* **33**, 665–670 (2010).
6. Chiti, F. & Dobson, C.M. Protein misfolding, functional amyloid, and human disease. *Annu. Rev. Biochem.* **75**, 333–366 (2006).
7. Rochet, J.C. & Lansbury, P.T. Amyloid fibrillogenesis: themes and variations. *Curr. Opin. Struct. Biol.* **10**, 60–68 (2000).
8. Inouye, H., Sharma, D., Goux, W.J. & Kirschner, D.A. Structure of core domain of fibril-forming PHF/Tau fragments. *Biophys. J.* **90**, 1774–1789 (2006).
9. Gazit, E. A possible role for π-stacking in the self-assembly of amyloid fibrils. *FASEB J.* **16**, 77–83 (2002).
10. Makin, O.S. & Serpell, L.C. Structures for amyloid fibrils. *FEBS J.* **272**, 5950–5961 (2005).
11. Gazit, E. Global analysis of tandem aromatic octapeptide repeats: the significance of the aromatic-glycine motif. *Bioinformatics* **18**, 880–883 (2002).
12. Reches, M., Porat, Y. & Gazit, E. Amyloid fibril formation by pentapeptide and tetrapeptide fragments of human calcitonin. *J. Biol. Chem.* **277**, 35475–35480 (2002).
13. Reches, M. & Gazit, E. Casting metal nanowires within discrete self-assembled peptide nanotubes. *Science* **300**, 625–627 (2003).
14. Tjernberg, L.O. *et al.* Arrest of β-amyloid fibril formation by a pentapeptide ligand. *J. Biol. Chem.* **271**, 8545–8548 (1996).
15. Soto, C. β-sheet breaker peptides inhibit fibrillogenesis in a rat brain model of amyloidosis: implications for Alzheimer's therapy. *Nat. Med.* **4**, 822–826 (1998).

16. Hörster, F. *et al.* Phenylalanine reduces synaptic density in mixed cortical cultures from mice. *Pediatr. Res.* **59**, 544–548 (2006).
17. Makin, O.S., Atkins, E., Sikorski, P., Johansson, J. & Serpell, L.C. Molecular basis for amyloid fibril formation and stability. *Proc. Natl. Acad. Sci. USA* **102**, 315–320 (2005).
18. Brooks, B.R. *et al.* CHARMM: the biomolecular simulation program. *J. Comput. Chem.* **30**, 1545–1614 (2009).
19. Haberthür, U. & Caflisch, A. FACTS: fast analytical continuum treatment of solvation. *J. Comput. Chem.* **29**, 701–715 (2008).
20. Lesné, S. *et al.* A specific amyloid-β protein assembly in the brain impairs memory. *Nature* **440**, 352–357 (2006).
21. Abramov, E. *et al.* Amyloid-β as a positive endogenous regulator of release probability at hippocampal synapses. *Nat. Neurosci.* **12**, 1567–1576 (2009).
22. Shedlovsky, A., McDonald, J.D., Symula, D. & Dove, W.F. Mouse models of human phenylketonuria. *Genetics* **134**, 1205–1210 (1993).
23. Gazit, V., Ben-Abraham, R., Pick, C.G. & Katz, Y. β-Phenylpyruvate induces long-term neurobehavioral damage and brain necrosis in neonatal mice. *Behav. Brain Res.* **143**, 1–5 (2003).
24. Cordero, M.E., Trejo, M., Colombo, M. & Aranda, V. Histological maturation of the neocortex in phenylketonuric rats. *Early Hum. Dev.* **8**, 157–173 (1983).
25. Lashuel, H.A., Hartley, D., Petre, B.M., Walz, T. & Lansbury, P.T. Neurodegenerative disease: amyloid pores from pathogenic mutations. *Nature* **418**, 291 (2002).
26. Bucciantini, M. *et al.* Inherent toxicity of aggregates implies a common mechanism for protein misfolding diseases. *Nature* **416**, 507–511 (2002).
27. Solomon, B. Clinical immunologic approaches for the treatment of Alzheimer's disease. *Expert Opin. Investig. Drugs* **16**, 819–828 (2007).
28. Schenk, D. *et al.* Immunization with amyloid-β attenuates Alzheimer-disease-like pathology in the PDAPP mouse. *Nature* **400**, 173–177 (1999).

Acknowledgments

We thank R. Shaltiel-Karyo for confocal microscopy analysis, S. Wolf for the electron diffraction analysis, L. Buzhansky for help with the NMR and HPLC analysis, J. Delarea for help with TEM and SEM experiments, Z. Barkay for help with the SEM and ESEM analysis, S.-C. Jung (Ewha Womans University, Korea) for BTBR-*Pah*^{enu2} mouse plasma and tissue samples, C. Troakes (London Neurodegenerative Diseases Brain Bank, King's College London and part of BrainNet Europe) and T. Arzberger (Centre for Neuropathology and Prion Research, München) for brain tissue samples, I. Benhar and members of the Gazit laboratory for helpful discussions. L.A.-A. gratefully acknowledges the support of the Colton Foundation. This work was partly supported by the Israel Science Foundation–Legacy Heritage Biomedical Science Partnership grant 862/09 and the Alzheimer's Association grant NIRG-11-205535 (to D.F.). The work in the A.C. group was supported by the Swiss National Science Foundation.

Author contributions

L.A.-A., O.C. and E.G. conceived and designed the experiments. L.A.-A. and L.V. planned and performed the experiments. D.T., L.V. and L.A.-A. designed and performed the mouse and human histology experiments. D.F. designed and coordinated the mice and human histology experiments. A.M. designed and performed the molecular dynamics simulations. A.C. designed and coordinated the molecular dynamics simulations. L.A.-A. and E.G. wrote the paper. All authors discussed the results and commented on the manuscript.

Competing financial interests

The authors declare no competing financial interests.

Additional information

Supplementary information is available in the online version of the paper. Reprints and permissions information is available online at http://www.nature.com/reprints/index.html. Correspondence and requests for materials should be addressed to E.G.